EUROPEAN FUSION DEVELOPMENT AGREEMENT

EFDA-JET-CP(05)02-41

A. Huber, P. Andrew, P. Coad, G. Corrigan, K. Erents, W. Fundamenski,
V. Huber, S. Jachmich, A. Korotkov, G.F. Matthews, Ph. Mertens, V. Philipps,
R. Pitts, J. Rapp, B. Schweer, G. Sergienko, M. Stamp
and JET EFDA contributors

Modelling JET Divertor Physics with the EDGE2D Code

Modelling JET Divertor Physics with the EDGE2D Code

A. Huber[1], P. Andrew[2], P. Coad[2], G. Corrigan[2], K. Erents[2], W. Fundamenski[2], V. Huber[1], S. Jachmich[3], A. Korotkov[2], G.F. Matthews[2], Ph. Mertens[1], V. Philipps[1], R. Pitts[4], J. Rapp[1], B. Schweer[1], G. Sergienko[1], M. Stamp[2] and JET EFDA contributors*

[1]*Institut für Plasmaphysik, Forschungszentrum Jülich GmbH, EURATOM Association, Trilateral Euregio Cluster, D-52425 Jülich, Germany*
[2]*Euratom/UKAEA Fusion Association, Culham Science Centre, Abingdon, Oxon OX14 3DB,†UK*
[3]*Laboratory for Plasmaphysics, ERM/KMS, Association EURATOM-Belgian State, Brussels, Belgium*
[4]CRPP, Association EURATOM-ConfÈdÈration Suisse, EPFL, Lausanne, Switzerland
** See annex of J. Pamela et al, "Overview of JET Results ", (Proc.20 th IAEA Fusion Energy Conference, Vilamoura, Portugal (2004).*

Preprint of Paper to be submitted for publication in Proceedings of the EPS Conference,
(Tarragona, Spain 27th June - 1st July 2005)

INTRODUCTION

Most single-null divertor tokamak experiments show strong in-out asymmetries in particle and heat fluxes connected to asymmetries in divertor density, temperature and radiation. As shown in many divertor tokamaks [1-4] and recently on JET [5,6], the imbalances strongly depend on the direction of the toroidal magnetic field (B_T) and are thus most probably a result of particle cross-field drifts. Experimentally observed outer-inner divertor power asymmetry P_T^{outer}/P_T^{inner} could not be explained by the asymmetry in the tomographically resolved divertor radiation alone [6]. Unequal power sharing between the two targets is most likely caused by the larger outboard area, enhanced radial transport on low field side (which is independent of the **B**×∇B-direction), and classical drift effects which reverse with the **B**×∇B-direction. This contribution presents analysis of experimental results using the EDGE2D/NIMBUS code.

1. RESULTS OF MODELLING

A pair of matched L-mode density limit discharges in forward and reversed toroidal field configurations have been modelled with the EDGE2D/NIMBUS simulation codes. EDGE2D solves the fluid equations for conservation of particles, momentum and energy for hydrogenic and impurity ions (all charge states), while neutrals are followed with the Monte-Carlo module NIMBUS. The code includes classical drifts (**E**×**B**, curvature, etc.), relevant atomic and molecular physics (ionisation, charge-exchange, recombination, etc.), impurity radiation from each charge state, and both physical and chemical sputtering of the divertor target plates.

Poloidally and radially uniform transport coefficients are chosen as $D_\perp=0.5m^2/s$ and $\chi_\perp=1m^2/s$ for particle and energy respectively. Simulations with these coefficients (for both field directions) are in good agreement with the measured radial density (see Fig.1) and temperature profiles. Both physical [7] and chemical sputtering [8] of carbon were enabled in the simulation. The plasma density was raised steadily to the density limit by gas fuelling into the inner leg of the divertor at constant input power (P_{heat}).

Figure 2 presents the simulated and experimental dependences of the divertor power asymmetry on the power entering the SOL (P_{SOL}). In the experiment, the NBI power was increased from 2MW to 8MW in two matched L-mode discharges with forward and reversed magnetic field configurations. The target power was measured using transient analysis of the thermocouple (TC) time traces. EDGE2D modelling shows that the geometry effects (the larger outboard area alone) lead to $P_T^{outer}/P_T^{inner} \sim 2-3$, which compares well with the observed value of ~ 2.2. With **B**×∇B down, the simulated asymmetry increases up to ~ 5 with the power entering the SOL, whereas with **B**×∇B up, it decreases to ~1.8, in agreement with experimental observation. This indicates that classical (poloidal) drifts are indeed responsible for the observed variation in P_T^{outer}/P_T^{inner}. Analysis with EDGE2D/NIMBUS indicates that such a power asymmetry may be the result of drifts such as **E**×**B** and **B**×∇T (poloidal components), the relative contribution of which scales as

ρ_θ / λ_T, where ρ_θ is the ion poloidal gyro-radius and λ_T is the characteristic length for temperature. The effect of ion ∇B (and centripetal) drifts was found to be negligible in this simulation.
Comparison of the results of simulations with experimental values (L-mode, density limit experiment, B_T=2.4T, I_p=1.7MA and an additional NBI-power of 2.5MW) for the absolute value of target power has also been performed and the results are summarised in Fig.3. Because the code does not include heating of the divertor via radiation ($P_{rad\_on\_tiles}$), this heating term was subtracted from the target power measured by an infrared camera (P_{IR}). The bolometer system provides complete plasma coverage and was used for tomographic reconstruction of the distribution of total radiation and correspondingly for evaluation of $P_{rad\_on\_tiles}$. One sees that the simulated absolute target power matches the measured one well. The power jump in the simulation at $n_e = 2.95\times10^{19}m^{-3}$ is not yet understood and further investigations are required.

The effect of different drift terms on the electron density profiles in inner and outer divertor can be seen in Fig.4. Simulation without drifts gives similar maximum densities in both divertor legs. The inclusion of all drifts into the simulation leads to a strong asymmetry in divertor density: higher density in inner and lower n_e in outer divertor. As can be seen in Fig.4, the n_e-asymmetry can be explained by the effect of a radial **E**×**B** drift and of the poloidal drift in the private flux region (the particle flow points from outer to inner divertor in the **B**×∇B$\downarrow$ case, and this flow direction reverses in reversed field configuration). Once again, the effect of ion ∇B(and centripetal) drifts was negligible. The inner and outer density and temperature have been also modelled with both the EDGE2D and the SOLPS fluid SOL plasma simulation codes in [9] and results from both codes match quite well the experiments.

Figure 5 presents the simulated and experimental values of D_α-emissions for two n_e. At a density of $n_e = 2.55\times10^{19}m^{-3}$ both legs are attached. Whereas at higher density of $n_e = 3.3\times10^{19}m^{-3}$ the outer leg is still attached, the inner divertor has reached the detachment phase. EDGE2D simulations successfully reproduce the D_α emission profile under attached conditions for both field configuration. On the other hand it shows underestimated value of D_α light in the inner divertor leg during the detachment phase. Additionally, EDGE2D simulations successfully describe CIII-emission profiles, both for discharges with forward and reversed field directions (not shown in the figure).

Although EDGE2D successfully reproduces the anticipated parallel pressure drop accompanying divertor detachment, it strongly underestimates the divertor D_α light, and cannot reproduce the gradual plasma flux reduction (roll-over behaviour) observed under detached conditions [10]. Figure 6 on the right shows the calculated outer and inner divertor ion flux. The values in Fig.6 indicate the H_γ/H_α ratios for both divertor legs. This ratio remains constant in the outer divertor during the whole density limit discharge simulation; it increases continuously from 0.025 to 0.042 in the inner leg, indicating the presence of strong recombination there. On the left side of Fig.6 the calculated saturation current profiles have been compared with the experiment. Once again, the strong deviation between modeling and experiment has been observed in the inner leg during detachment. Since the code cannot explain the drop in total ion flux to the divertor, further investigations of ion-flux detachment are required.

CONCLUSION

EDGE2D calculations with drifts successfully describe out-in target heat power asymmetry, both for discharges with forward and reversed field directions. Also the absolute target power could be well predicted during the whole phase of density limit L-mode discharges. The effect of **E×B** drifts was found to be dominant, on the other hand the effect of ion ∇B (and centripetal) drifts was negligible. In addition, the EDGE2D simulations successfully reproduce the observed asymmetries in divertor density and electron temperature, and the atomic carbon (CIII) emission profiles; on the other hand, the D_α emission profile was well matched only under attached conditions. Whereas EDGE2D successfully reproduces the anticipated parallel pressure drop accompanying divertor detachment, it strongly underestimates the divertor D_α light, and cannot reproduce the gradual plasma flux reduction (roll-over behaviour) observed under detached conditions.

REFERENCES

[1]. F.Wagner, M.Keilhacker and the ASDEX and NI Teams, J. Nucl. Mater. 121 (1984) 103.

[2]. D.N. Hill.et al., J. Nucl. Mater. 176-177 (1990) 158.

[3]. N. Asakura et al., J. Nucl. Mater. 220-222 (1995) 395.

[4]. I.H. Hutchinson et al, Plasma Phys. Control. Fusion 38 (1996), A301.

[5]. R.A. Pits et al., J. Nucl. Mater. 337-339 (2005) 146

[6]. A. Huber et al., J. Nucl. Mater. 337-339 (2005) 241.

[7]. W. Eckstein et al., Report IPP9/82, IPP, Garching (1993)

[8]. A.A. Haasz et al., J. Nucl. Mater. 248 (1997), 19.

[9]. X. Bonnin et al., this conference, paper reference number P2.110

[10]. P.C. Stangeby, The Plasma Boundary of Magnetic Fusion Devices, Institute of Physics (2000)

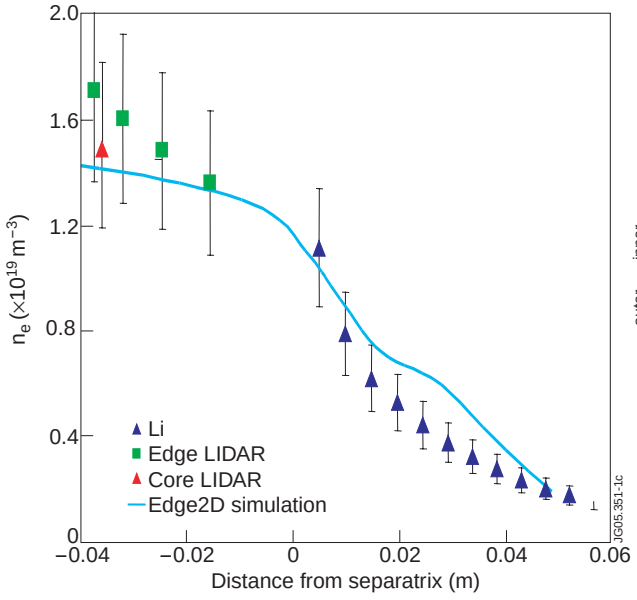

Figure 1: Edge density profiles from EDGE2D compared with various diagnostics.

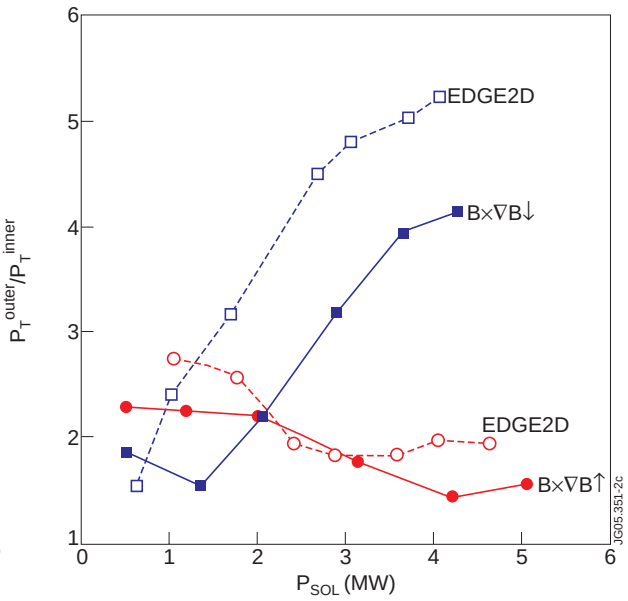

Figure 2: Experimental and simulated divertor power asymmetries versus P_{SOL} for forward and reversed field directions.

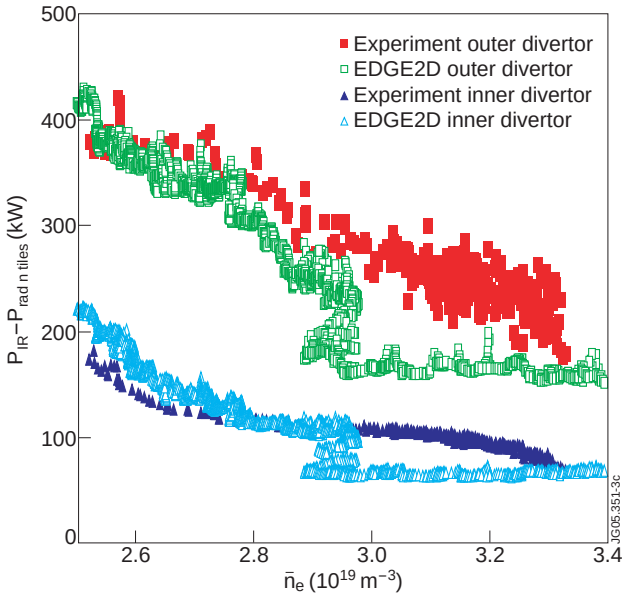

Figure 3: Experimental and simulated absolute target power versus central averaged density for the forward field configuration.

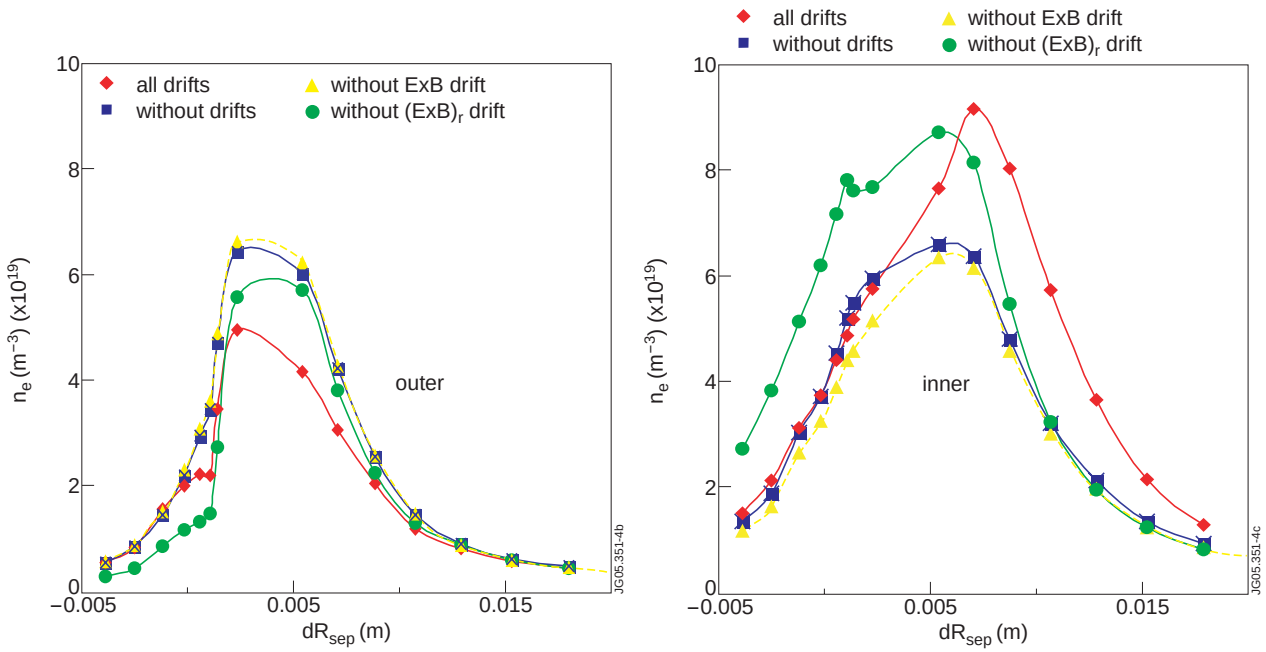

Figure 4: The effect of different drift terms on the electron density profiles in inner and outer divertor.

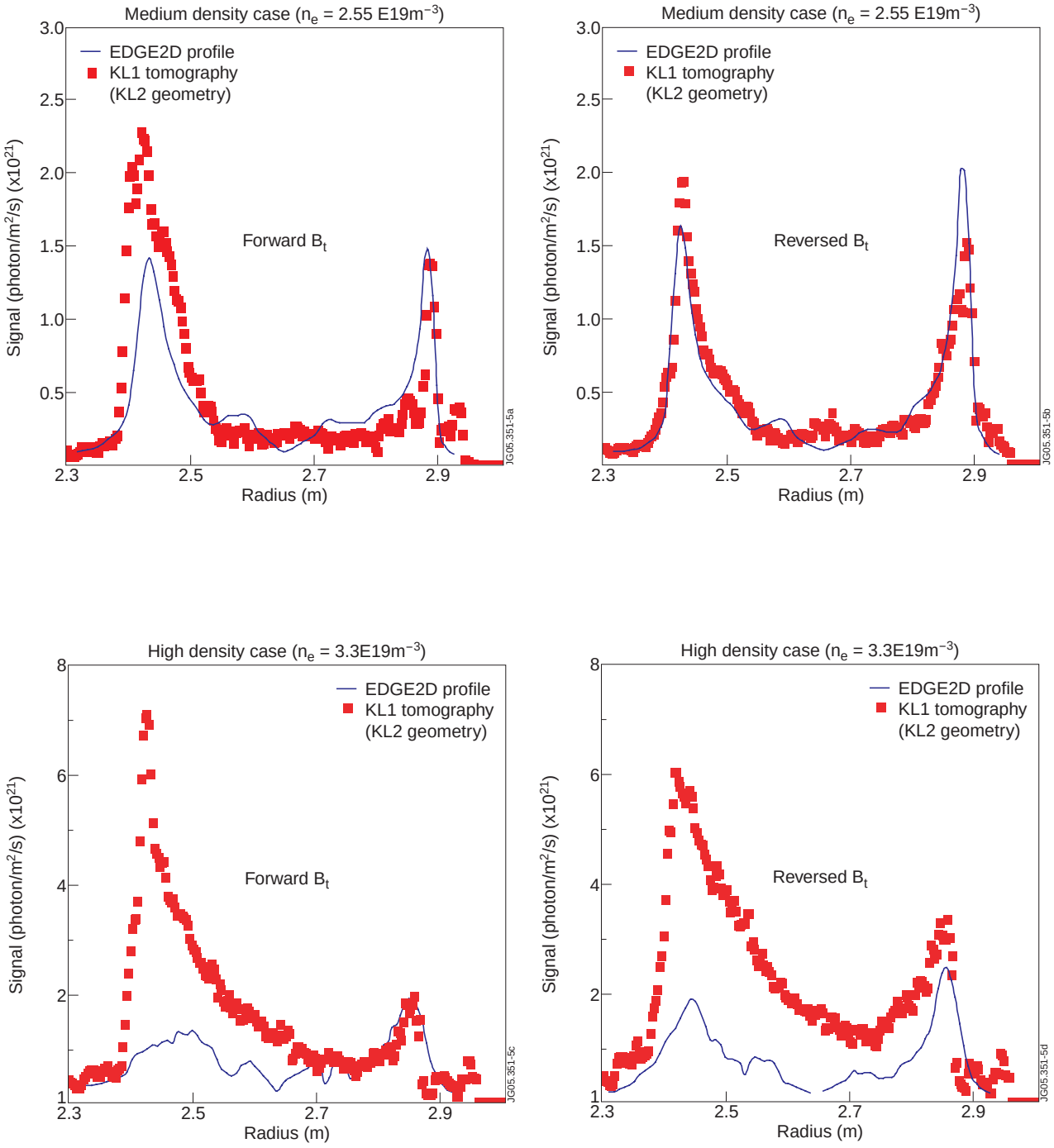

Figure 5: Comparison of simulated and mesured D_a-emissions profiles for two different field directions and two different electron densities.

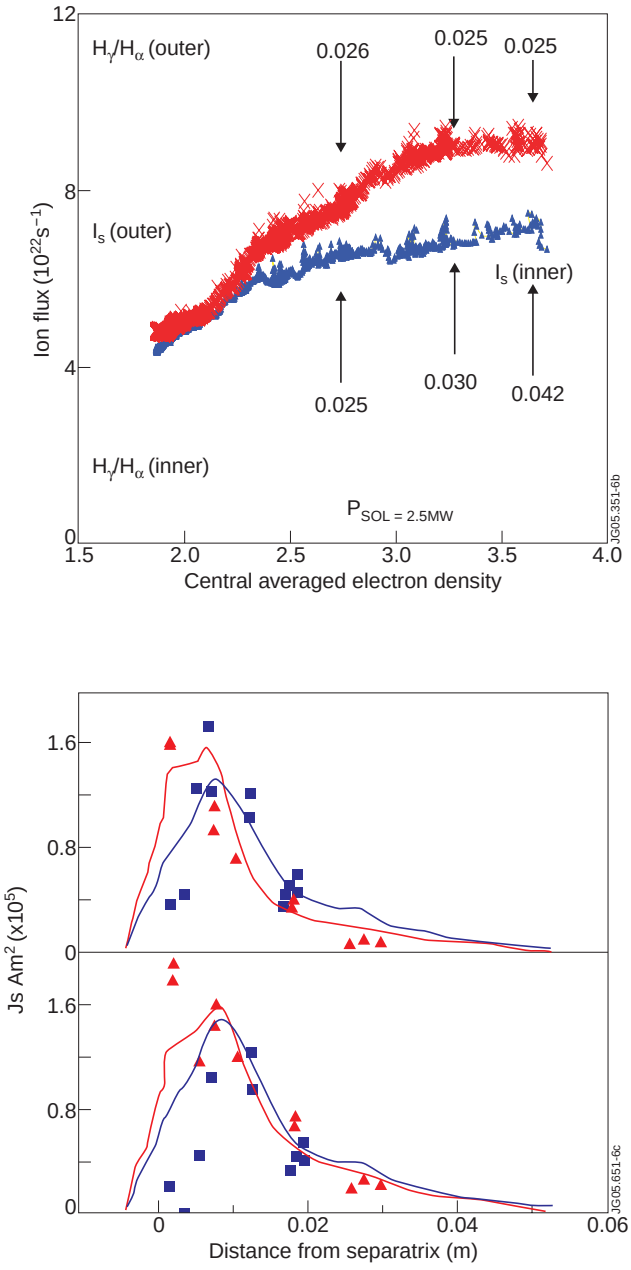

Figure 6: Comparison of simulated and measured Js-profiles (top) and calculated outer and inner ion flux (bottom) for a "density limit" discharge.